Received: 15 October 2020 | Revised: 17 March 2021 | Accepted: 15 April 2021

DOI: 10.1002/ar.24680

SPECIAL ISSUE ARTICLE

The Anatomical Record | WILEY

Cochlear apical morphology in toothed whales: Using the pairing hair cell—Deiters' cell as a marker to detect lesions

Maria Morell[1,2,3] | **Lonneke L. IJsseldijk**[4] | **Marina Piscitelli-Doshkov**[3] | **Sonja Ostertag**[5,6] | **Vanessa Estrade**[7] | **Martin Haulena**[8] | **Paul Doshkov**[9] | **Jérôme Bourien**[2] | **Stephen A. Raverty**[3,10] | **Ursula Siebert**[1] | **Jean-Luc Puel**[2] | **Robert E. Shadwick**[3]

[1]Institute for Terrestrial and Aquatic Wildlife Research, University of Veterinary Medicine Hannover, Foundation, Büsum, Germany

[2]Institute for Neurosciences of Montpellier, University of Montpellier, INSERM Unit 1051, Montpellier, France

[3]Department of Zoology, The University of British Columbia, Vancouver, British Columbia, Canada

[4]Division of Pathology, Department of Biomolecular Health Sciences, Faculty of Veterinary Medicine, Utrecht University, Utrecht, The Netherlands

[5]School of Public Health, University of Waterloo, Waterloo, Ontario, Canada

[6]Freshwater Institute, Fisheries and Oceans Canada, Winnipeg, Manitoba, Canada

[7]Association GLOBICE, Saint Pierre, La Reunion, France

[8]Vancouver Aquarium Marine Science Center, Vancouver, British Columbia, Canada

[9]Cape Hatteras National Seashore, Manteo, North Carolina

[10]Animal Health Center, Animal Health Center, Ministry of Agriculture, Abbotsford, British Columbia, Canada

Correspondence
Maria Morell, Institute for Terrestrial and Aquatic Wildlife Research, University of Veterinary Medicine Hannover, Foundation, 25761 Büsum, Germany.
Email: maria.morell@tiho-hannover.de

Funding information
Canadian Natural Sciences and Engineering Research Council Accelerator, Grant/Award Number: RGPAN 312039-13; Canadian Natural Sciences and Engineering Research Council Discovery, Grant/Award Number: RGPAS 446012-13; Marie Skłodowska-Curie Individual Post-doctoral Fellowship, Grant/Award Number: 751284-H2020-MSCA-IF-2016

Abstract

The apex or apical region of the cochlear spiral within the inner ear encodes for low-frequency sounds. The disposition of sensory hair cells on the organ of Corti is largely variable in the apical region of mammals, and it does not necessarily follow the typical three-row pattern of outer hair cells (OHCs). As most underwater noise sources contain low-frequency components, we expect to find most lesions in the apical region of the cochlea of toothed whales, in cases of permanent noise-induced hearing loss. To further understand how man-made noise might affect cetacean hearing, there is a need to describe normal morphological features of the apex and document interspecific anatomic variations in cetaceans. However, distinguishing between apical normal variability and hair cell death is challenging. We describe anatomical features of the organ of Corti of the apex in 23 ears from five species of toothed whales (harbor porpoise *Phocoena phocoena*, spinner dolphin *Stenella longirostris*, pantropical spotted dolphin *Stenella attenuata*, pygmy sperm whale *Kogia breviceps*, and beluga whale *Delphinapterus leucas*) by scanning electron microscopy and immunofluorescence. Our results showed an initial region where the lowest frequencies are encoded with two or three rows of OHCs, followed by the

typical configuration of three OHC rows and three rows of supporting Deiters' cells. Whenever two rows of OHCs were detected, there were usually only two corresponding rows of supporting Deiters' cells, suggesting that the number of rows of Deiters' cells is a good indicator to distinguish between normal and pathological features.

KEYWORDS

apex, apical region, cochlea, Deiters' cells, hair cells, toothed whales

1 | INTRODUCTION

There is an increasing concern about the effects of underwater noise pollution on marine mammals (Erbe, Dunlop, & Dolman, 2018; Simmonds et al., 2014). Hearing is essential to cetaceans since sound is used for finding prey, communication, or navigation. Thus, changes to their hearing system may have a large impact on their ability to perform vital activities. In terrestrial mammals, if an individual is exposed to a high intensity audible sound for a certain duration, structural alterations can occur in the sensory cells of the organ of Corti as a result of mechanical damage and metabolic fatigue (Lim & Dunn, 1979).

Most underwater noise sources that are potentially damaging for marine mammals have major low frequency components (National Research Council, 2003), overlapping with the lowest frequencies of the hearing range in toothed whales. These low frequency sources include oil and gas exploration and exploitation activities, geophysical surveys or low frequency active sonar. As a result, we anticipate potential lesions associated with underwater noise exposure in cetaceans to occur most commonly in the region of the cochlea where the lowest frequencies of their hearing range are encoded, that is, the apex (or apical region) of the cochlea.

Typically, the organ of Corti in mammals is comprised of sensory cells and supporting cells (Figure 1, see Lim, 1986 for review). There are two types of sensory cells, inner hair cells (IHCs) and outer hair cells (OHCs), which are arranged in three parallel rows, amplify the incoming signal and are responsible for frequency sensitivity and selectivity. IHCs are aligned in one row and they transduce the mechanical sound stimulation into the release of neurotransmitter to the Type I afferent neurons that conduct the auditory information to the brain stem. There are several types of supporting cells that are highly differentiated epithelial cells and

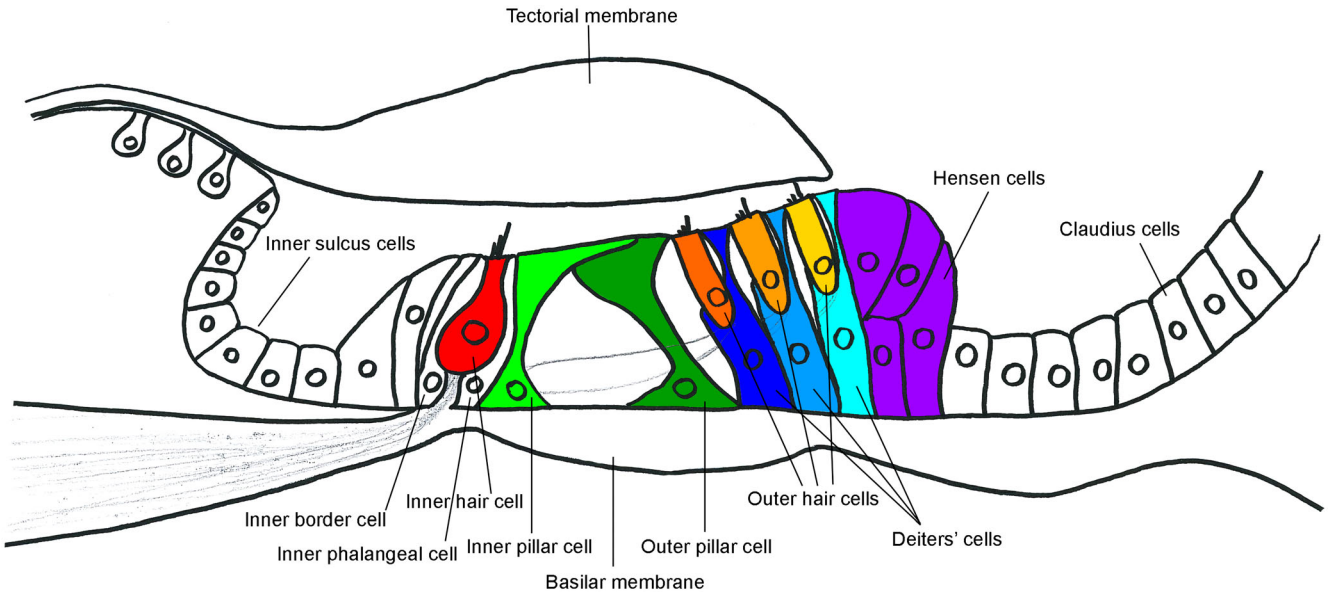

FIGURE 1 Schematic representation of the sensory cells and supporting cells of the organ of Corti. The colors used to highlight the sensory cells and some types of supporting cells correspond to the legend of Figures 4, 5, 6, and 9

form the reticular lamina. The supporting cells are called (from medial to lateral): inner sulcus cells, inner border cells, inner phalangeal cells, inner pillar cells, outer pillar cells, Deiters' cells, Hensen cells, and Claudius cells (Figure 1, see Raphael & Altschuler, 2003 and Monzack & Cunningham, 2013 for review). Besides providing structural support (Slepecky, Henderson, & Saha, 1995), the supporting cells participate in the recycling process of K^+ back to the endolymph space, which is required for hearing (Kikuchi, Adams, Miyabe, So, & Kobayashi, 2000; Spicer & Schulte, 1998). The Deiters' cells are arranged in three parallel rows and they are in contact with the basilar membrane and the basal domain of the OHCs, forming a "seat" for OHCs. In addition, Deiters' cells have a phalangeal process that contributes to the reticular lamina mosaic, filling the spaces between OHCs. The first row of Hensen cells are also referred to as Tectal cells and are not in contact with the basilar membrane (Henson, Jenkins, & Henson, 1983; Spicer & Schulte, 1994). However, for this manuscript, Tectal and Hensen cells will not be differentiated.

Typically, structural alterations as a consequence of noise exposure include changes in the stereocilia and degeneration and loss of entire hair cells, among others (Bredberg, Ades, & Engstrom, 1972; Engstrom, Borg, & Canlon, 1984; Hu, Guo, Wang, Henderson, & Jiang, 2000). Following cochlear hair cell death, neighboring supporting cells initiate the elimination of the hair cell, leaving a distinct scar. This "scarring" process results in the simultaneous expansion and sealing of the reticular lamina (Lim & Dunn, 1979; Lim & Melnick, 1971) as a rapid protective response to hair cell apoptosis and is not equivalent to tissue scar formation as in wound healing. There are several structural alterations observed regularly in cetacean cochlea, such as fusion of the stereocilia of the sensory cells, bleb formation, perforations of the reticular lamina, or swelling of the dendrites. However, these alterations are not considered pathological features but rather a consequence of postmortem decomposition in our samples due to a delay between the death of the individual and the fixation of the inner ear (Morell et al., 2015). Consequently, when describing the normal (i.e., undamaged) morphology of the cells of the organ of Corti in cetacean species in this study, we will only focus on the disposition of hair cells and supporting cells, but do not take into account other alterations that can lead to temporary and permanent hearing loss in mammals (Bredberg et al., 1972; Saunders, Dear, & Schneider, 1985). However, hair cell death by apoptosis and scar formation can be distinguished and considered as pathological features. The presence of scarring among hair cell rows is therefore an important criterion for assessing possible history of noise-induced cochlear lesions that can be distinguished from artifacts that may derive from tissue autolysis (Morell et al., 2015; Morell et al., 2017).

In terrestrial mammals, the hair cell disposition in the apex of the cochlea is variable (Lenoir, Puel, & Pujol, 1987). Whereas, hair cells within the rest of the organ of Corti (i.e., organ of Corti excluding the apex) typically appear as a single row of IHCs and three rows of OHCs. In several species of bats, it is common to find two rows of OHCs (Vater & Lenoir, 1992) or locations with fewer OHCs in the apex (Vater & Siefer, 1995). One of the most extreme anatomic variations is reported in the mole rat *Spalax ehrenbergi*. In this low frequency specialist, the first uppermost half turn of the cochlea is formed only by IHCs, while OHCs are absent (Raphael, Lenoir, Wroblewski, & Pujol, 1991).

There are some studies of the cochlear sensory epithelium in toothed whales (Girdlestone et al., 2018; Morell et al., 2015; Morell et al., 2017; Morell, Raverty, et al., 2020; Morell, Vogl, et al., 2020; Wever, McCormick, Palin, & Ridgway, 1971a, 1971b; Wever, Ridgway, Palin, & McCormic, 1972) focusing on describing anatomical features, structural adaptations and morphometric variations of the organ of Corti along the cochlear spiral in harbor porpoises (*Phocoena phocoena*), striped dolphins (*Stenella coeruleoalba*), bottlenose dolphins (*Tursiops truncatus*), Atlantic white-sided dolphins (*Lagenorhynchus acutus*), and beluga whales (*Delphinapterus leucas*). However, to the best of our knowledge, no previous reports have described the arrangement of hair cells in the apex of the cochlea. This is most likely because these cells are more susceptible to postmortem decomposition than the cells of the organ of Corti of the base, possibly related to their ultrastructural characteristics, that is, the cytoskeleton of hair cells and supporting cells of the apex of toothed whales is not as highly developed as observed in the base of the cochlea (Morell et al., 2015).

Herein, we present the first detailed baseline study of cochlear apical morphology for five species of toothed whales: harbor porpoise (*P. phocoena*), spinner dolphin (*Stenella longirostris*), pantropical spotted dolphin (*Stenella attenuata*), pygmy sperm whale (*Kogia breviceps*), and beluga whale (*D. leucas*). The "normal" morphology and interspecific and intraspecific variability of the hair cell disposition in the apex of the cochlea of cetaceans will be important for diagnosis of potential noise-induced hearing loss in future cases.

For the purposes of this study, we will define the apex as the first millimeter of the cochlear spiral, measured along the limit between the first row of OHCs and the

inner pillar cells. Here, the sensory epithelium of the apex of these odontocete species is described by scanning electron microscopy (SEM) and by immunofluorescence (IF).

2 | MATERIALS AND METHODS

2.1 | Sample collection

Twenty-three years from five odontocete species were perfused perilymphatically between 1.25 and 18 hr postmortem using either 10% neutral buffered formalin, 2.5% glutaraldehyde (in 0.1 M phosphate buffer or in 0.1 M cacodylate buffer), or 4% paraformaldehyde in PBS, following the protocol described by Morell and André (2009). Specifically, cochleas were collected and preserved from harbor porpoise ($n = 11$ ears from 10 individuals), spinner dolphin ($n = 1$ ear), pantropical spotted dolphin ($n = 2$ ears from 1 individual), pygmy sperm whale ($n = 1$ ear), and beluga whale ($n = 8$ ears from 5 individuals). The variability of fixation delay was due to the opportunistic nature of cetacean samples. Studying the cochlea of neonates is ideal since they would most likely show normality given they are least likely to have encountered any agent that might cause hair cell loss. However, we also included juveniles and adults when the apex was well preserved, which is essential to account for the variability within a species throughout the life of an individual. Table 1 details the origin and species of the processed samples, postmortem interval, analysis techniques, ear (right or left), and field identification number.

All species were transferred using CITES permits and all required permits for the belugas were obtained from the Aurora Research Institute License No. 15467, Department of Fisheries and Oceans Fishing License No. S-14/15-3019-YK, Marine Mammal Transport License #18843, and Environmental Impact Screening Committee (EISC) #03-14-03.

2.2 | Sample preparation

The periotic bone surrounding the cochlea was decalcified by immersion in 14% ethylenediaminetetraacetic acid tetrasodium salt hydrate, pH 7.4, at room temperature (changing the solution once every 7–10 days; Callis & Sterchi, 1998) or the rapid decalcifier RDO (Apex Engineering Products Corporation, Aurora, IL). Concentrations of 50% RDO for the first 24 hr and 25% RDO in the following days were used, following a previously optimized protocol (Morell, Degollada, Alonso, Jauniaux, & Andre, 2009).

2.3 | Scanning electron microscopy

The decalcification of the periotic bone was stopped when the vestibular scala and the stria vascularis of the cochlea were exposed. Subsequently, the cochleas and their tectorial membranes were dissected, dehydrated with increasing concentrations of ethanol, critical point dried with CO_2, and coated with gold, gold–palladium or platinum–palladium. The samples were observed with an SEM at the University of British Columbia Bioimaging Facility, Canada (Hitachi S-4700), at the COMET, Montpellier Resources Imagery, France (Hitachi S-4000), and at the Institut Européen des Membranes (IEM), France (Hitachi S-4800).

2.4 | Immunofluorescence

The ears used for IF were further decalcified until the vestibular, cochlear and tympanic scala were exposed. The methodology followed for IF is described in detail in Morell, Vogl, et al. (2020). In short, the cochleas were dissected using the whole-mount technique until flat preparations of half turns were obtained. Then, the segments were blocked with 5% normal donkey serum for 1 hr and incubated overnight at 4°C with the following primary antibodies: goat anti-prestin (Santa Cruz SC-22692, 1:200) for OHC labeling, rabbit anti-myosin VI (Proteus 25-6791, 1:500) for IHC and OHC labeling and mouse anti-neurofilament 200 (Sigma-Aldrich N0142, 1:400) or chicken anti-neurofilament H (Millipore AB5539, 1:5,000) for Type I innervation labeling. Anti-neurofilament antibodies labeling was not pertinent to the anatomical description of the hair cells of the sensory epithelium to this study. Thus, the results are not shown for most species in this study, only for pantropical spotted dolphin (Figure 6). The primary antibodies were washed three times (10 min each) with PBT (0.1% triton-X 100 with 2 mg/L bovine serum albumin in PBS), incubated with secondary antibodies for 2 hr in the dark at room temperature (Molecular Probes A11055, A10042, and A31571, Sigma-Aldrich SAB4600127, 1:400 dilution), and incubated for 30 min with DAPI (Thermo Scientific 62248, 1:1,000 dilution) to counter-stain the nucleus. In one cochlea, F-actin of the cells of the organ of Corti was labeled with phalloidin (FluoProbes X5 505 FP-AZ0130, 10 nanomoles in 1.5 ml initially, 1:100 dilution), which was added to the secondary antibody solution. The whole-mounts were subsequently washed three times (10 min each) with PBS, treated with 0.2% Sudan Black B (except for the sample labeled with phalloidin) for 10 min to reduce the fluorescence of the tissue, and rinsed three times (1 min each) with 70% ethanol. Then,

TABLE 1 Detailed breakdown of the inner ear samples processed for this study, including species, origin, age group, sex, processing technique, number of hours between death and fixation of the cochlea, and whether there was complete or partial information of the first millimeter of the cochlea

Id number	Ear (R, L)	Species	Origin	Age group	Total length (cm)	Sex	Hours between death and fixation	Analysis technique	Information from the apex
Cet 351B_UT 1318	L	Harbor porpoise	The Netherlands	N	79.5	M	3.5 hr	SEM	Partial (0–360 and 720–1,000 μm)
cet 355B_UT 1341	L	Harbor porpoise	The Netherlands	J	113	F	5 hr	SEM	Partial (0–60 and 480–1,000 μm)
cet 401A_ Pp02	R	Harbor porpoise	The Netherlands	A	147	M	16 hr	SEM	Partial (600–1,000 μm)
cet 404A_UT 1495	R	Harbor porpoise	The Netherlands	J	105	M	4 hr	SEM	Partial (0–100 and 600–1,000 μm)
cet 404B_UT 1495	L	Harbor porpoise	The Netherlands	J	105	M	4 hr	IF	Complete
cet 405A_UT 1509	R	Harbor porpoise	The Netherlands	J	113	F	Approximately 6 hr	SEM	Partial (0–240 μm)
cet 408A_UT 1518	R	Harbor porpoise	The Netherlands	J	107	F	6–18 hr	SEM	Partial (0–200 and 280–1,000 μm)
cet 410A_UT 1428	R	Harbor porpoise	The Netherlands	N	75	M	Approximately 12 hr	SEM	Partial (0–100 and 640–1,000 μm)
cet 411A_UT 1531	R	Harbor porpoise	The Netherlands	A	139	M	Approximately 10–12 hr	SEM	Partial (0–560 μm)
cet 415B_Jack	L	Harbor porpoise	Canada	A	156	M	9.5–11.5 hr	SEM	Complete
cet 426A_UT1562	R	Harbor porpoise	The Netherlands	J	99	M	4 hr	IF	Partial (80–1,000 μm)
cet 414A_SL 974_2016_49	R	Spinner dolphin	Réunion, France	N	83	M	6-12 hr	SEM	Complete
cet 446A_974_2018_01	R	Pantropical spotted dolphin	Réunion, France	J	115	F	2-3 hr	IF	Complete
cet 446B_974_2018_01	L	Pantropical spotted dolphin	Réunion, France	J	115	F	2-3 hr	SEM	Partial (20–100, 140–180, 260–620, 680–720 and 780–1,000 μm)
cet 434B_CAHA 385	L	Pygmy sperm whale	United States	A	249.5	M	2–3 hr	IF	Complete
cet 336A_HI-14-04	R	Beluga whale	Canada	A	409	M	3.25 hr	SEM	Partial (0–800 and 880–1,000 μm)
cet 340A_HI-14-08	R	Beluga whale	Canada	A	335	M	1.25 hr	IF	Complete
cet 340B_HI-14-08	L	Beluga whale	Canada	A	335	M	2.5 hr	SEM	Partial (120–1,000 μm)
cet 344A_HI-14-12	R	Beluga whale	Canada	A	406	M	2–3 hr	SEM	Complete
cet 344B_HI-14-12	L	Beluga whale	Canada	A	406	M	2–3 hr	SEM	Complete
cet 419A_Qila	R	Beluga whale	Canada	A	356	F	5.5 hr	IF	Partial (0–200 and 400–1,000 μm)
cet 419B_Qila	L	Beluga whale	Canada	A	356	F	6 hr	SEM	Partial (0–200 and 540–740 μm)
cet 420A_Aurora	R	Beluga whale	Canada	A	381	F	16 hr	IF	Partial (0–200 and 860–1,000 μm)

Abbreviations: A, adult; IF, immunofluorescence; J, juvenile; L, left; N, neonate, R, right; SEM, Scanning electron microscopy.

the segments were rinsed three times (10 min each) with PBS and mounted on a slide with 0.1% *N*-propyl gallate in 90% glycerol. The samples were then observed under an Olympus FV1000 confocal microscope at the University of British Columbia Bioimaging Facility (UBC, Vancouver, Canada) and a Zeiss LSM880 confocal microscope at the Montpellier Resources Imagery (MRI, Montpellier Cell Biology Research Center, France).

Small subsegments were randomly taken from other locations of the cochlea as controls. Control for nonspecific binding of the secondary antibodies was performed in all individuals: samples were incubated without primary antibodies, but with the same concentrations of the secondary antibody as the experimental segments (and DAPI in some cases). In most of the samples, there was also a specificity control, where the samples were incubated with the same concentration of IgG as the primary antibodies as the experimental segments (Sigma-Aldrich ref. I5256, M5284, and I5006), and incubated with the same concentrations of the secondary antibody and DAPI as the experimental segments. In most of the samples, there was a control for autofluorescence, where neither primary nor secondary antibodies were used.

For SEM and IF, the cochlear length measurements used to describe the organ of Corti cells of the first millimeter of the apex were made using ImageJ (National Institutes of Health) software. The brightness and contrast of the images used for the figures were enhanced with Adobe Photoshop (Adobe Systems Incorporated) software. For an easier comparison, some ears have been inverted horizontally to orient the beginning of the apex to the left of the figure.

2.5 | Statistical analysis

The disposition of the sensory cells along the apex was quantified in blocks of 20 μm of cochlear length (measured at the level of OHC1 in contact with the inner pillar cells). For each 20 μm of cochlear length, a code was assigned per sensory cell type, according to its apical membrane appearance. A presence was assigned 1, absence 0, and alternation 0.5 as there were some sensory cells detected in this specific row, and some were absent. We also highlighted those regions where the reticular lamina could not be assessed either due to autolysis, processing artifacts (e.g., shearing or folding of the basilar membrane) or deposition of cellular debris on the reticular lamina surface, which obscures the identification of the underlying cell types (Table 1, gray rectangles in Figures 2 and 3).

Averaged values along the apical ends of the cochlea of harbor porpoise and beluga were calculated per each block of 20 μm using MATLAB software (MathWorks, *nanmean* function) and excluding those anatomic locations that could not be evaluated (blue in Figures 2 and 3).

3 | RESULTS

3.1 | Harbor porpoise

Two of the eleven analyzed ears from harbor porpoises (one juvenile and one adult) provided complete information on the disposition of OHCs throughout the first millimeter of the apex. The remaining nine ears had regions where the sensory cells of the organ of Corti could not be assessed, due to either unintentional damage during dissection or processing, or because there was cellular debris on the surface of the reticular lamina, which obscured the sensory epithelium. Although there were areas in the cochlea of individual animals that could not be evaluated, there were at least five ears with sufficient overlapping information of a particular region to account for interindividual variability throughout the apex. Figure 2 shows a schematic representation of the results from all ears. The first zone contained two, three, or an alternation of two and three rows of OHCs in all the samples analyzed, which could extend from 220 up to 840 μm from the apex, with an average of 420 μm in at least 70% of the cases (Figures 2, 4, and 5). Beyond this range, the typical formation of three rows of OHCs was observed. In some porpoises, there were a few cells arranged in a fourth row of OHCs. The IHCs were not always well preserved, but when present (or a cavity in the tissue remained as an indication of their position antemortem) they were found consistently throughout the apex. There was high interindividual variability detected by SEM and IF.

Phalloidin labeling, which was possible with one cochlea that was fixed with 4% paraformaldehyde, proved to be ideal to differentiate among sensory and supporting cell types through the sensory epithelium. Figure 4c shows maximum projections from z-stacks of the organ of Corti and the different cell types were highlighted in colors in the phalloidin labeling channel.

Figure 5b highlights the arrangements of sensory and supporting cells in different colors in high magnification SEM micrographs. Figure 5d also contains information on the disposition of the cells of the organ of Corti in the middle turn, for comparison with the apex.

3.2 | Spinner dolphin

Although there was only one ear analyzed from spinner dolphin, the results are included because the well-

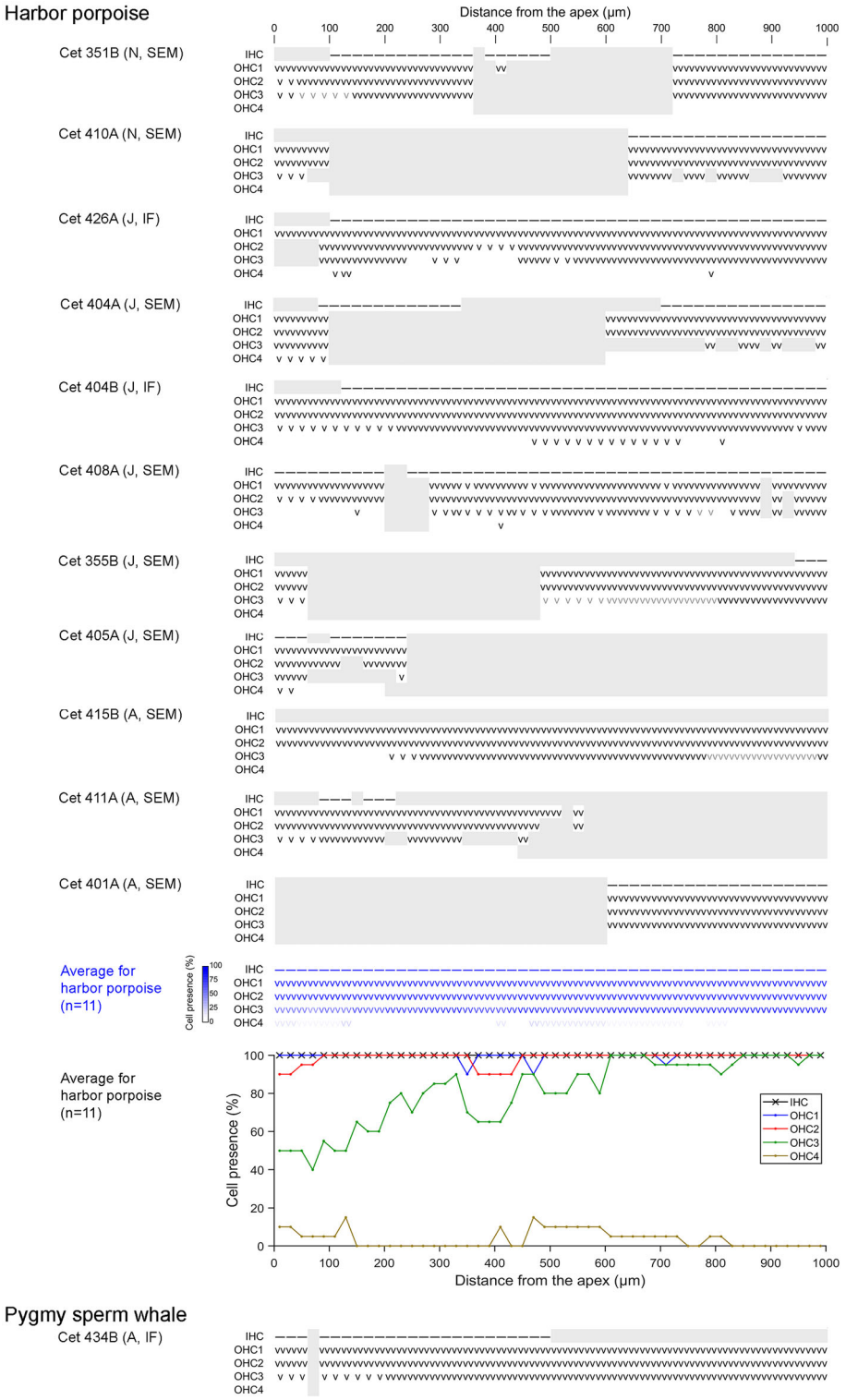

FIGURE 2 Schematic representation of the apex of the ears analyzed from harbor porpoise (*Phocoena phocoena*) and pygmy sperm whale (*Kogia breviceps*) for this study. The inner hair cells (IHCs) are labeled with a hyphen and the outer hair cells (OHCs) with a "V." The gray shading represents regions where there was no information due to decomposition, cellular debris on the surface of the organ of Corti that impeded the visualization of the cells, or due to unintentional damage during the dissection or processing of the sample. The gray "V" represents areas where there was partial information of sensory cells, or they showed signs of decomposition making hair cell identification challenging. It is possible that there was a first region with no information of the organ of Corti in the pygmy sperm whale since it was challenging to determine its beginning. The averaged values for harbor porpoise are shown in blue and include percentages of cell presence. This representation corresponds to about half of the number of sensory cells found in the first millimeter of the apex

preserved sample was from a neonate and had complete information of OHCs of the first millimeter of the apex. The SEM revealed that in the first 240 μm there was an alternation between two and three rows of OHCs, followed by an area of two rows of OHCs up to 560 μm from the apex. Another zone of transition occurred from 560 μm until 660 μm from the apex with two and three rows that was followed by the typical three-row alignment OHCs throughout the rest of the cochlea (Figures 3 and 6a). There was no information on the presence of IHCs due to postmortem decomposition (Figure 6a). Figure 6b shows the disposition of the OHCs and supporting cells in higher magnification.

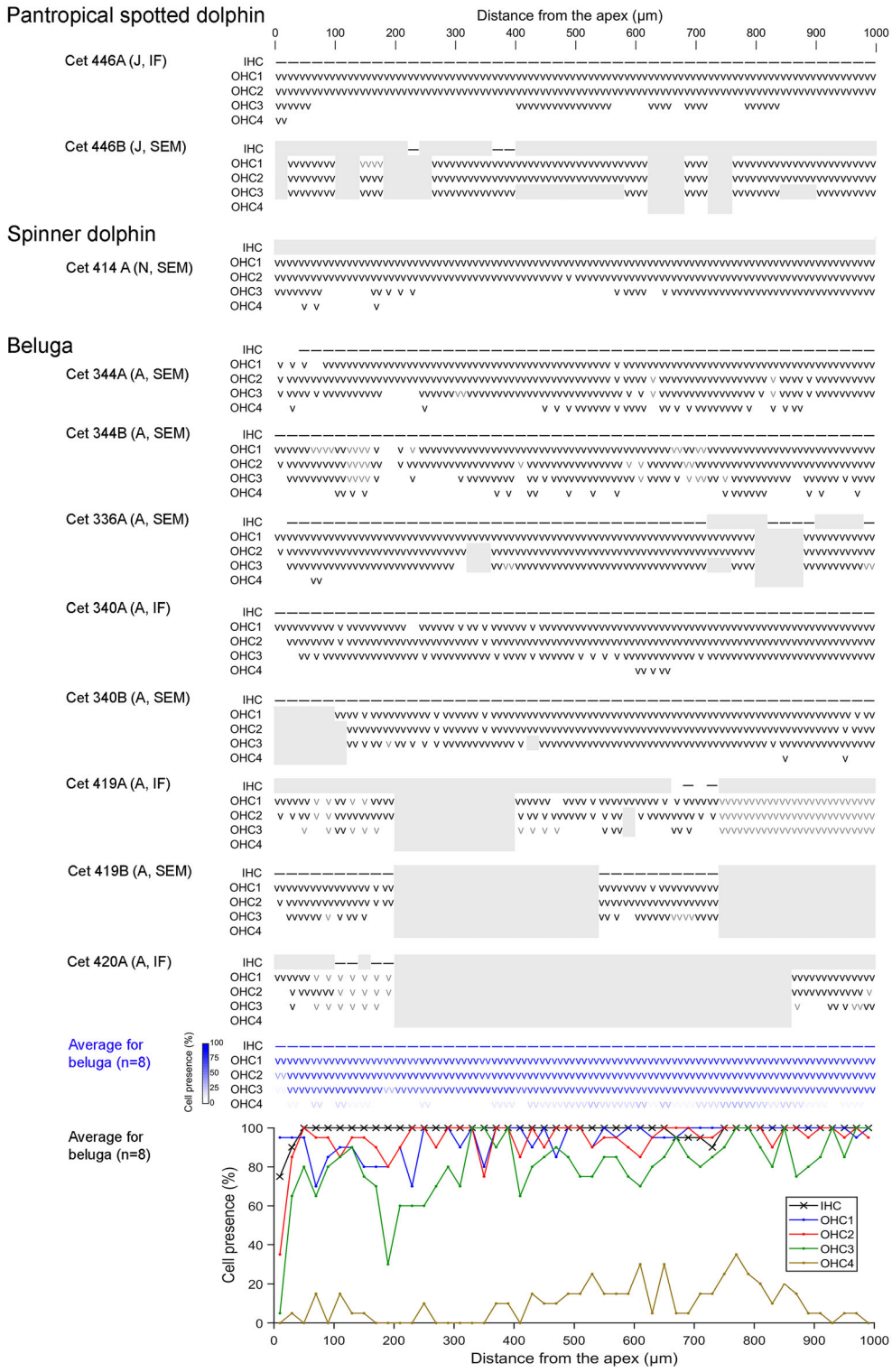

FIGURE 3 Schematic representation of the apex of the ears analyzed from pantropical spotted dolphin (*Stenella attenuata*), spinner dolphin (*Stenella longirostris*), and beluga whale (*Delphinapterus leucas*) for this study. The inner hair cells (IHCs) are labeled with a hyphen and the outer hair cells (OHCs) with a "V." The gray shading represents regions where there was no information, due to decomposition, cellular debris on the surface of the organ of Corti that impeded the visualization of the cells, or due to unintentional damage during the dissection or processing of the sample. The gray "V" represents areas where there was partial information of sensory cells, or they showed signs of decomposition making hair cell identification challenging. The averaged values for beluga are shown in blue and include percentages of cell presence. This representation corresponds to about half of the number of sensory cells found in the first millimeter of the apex

3.3 | Pantropical spotted dolphin

Two ears from the same individual were analyzed, the right ear with IF and the left ear with SEM. The dolphin was estimated to be a yearling with reasonably well preserved cochlea (Figure 7). The right ear had a complete apex (Figures 3 and 7a); whereas there was a lack of information on the sensory epithelium at around 220 μm and scattered throughout the apex of the left cochlea (Figure 3).

The results were different in both ears. While the right ear had an alternation of three and two rows of OHCs throughout the apex, the left ear featured a uniform three-row pattern of OHCs from 260 μm onward. In

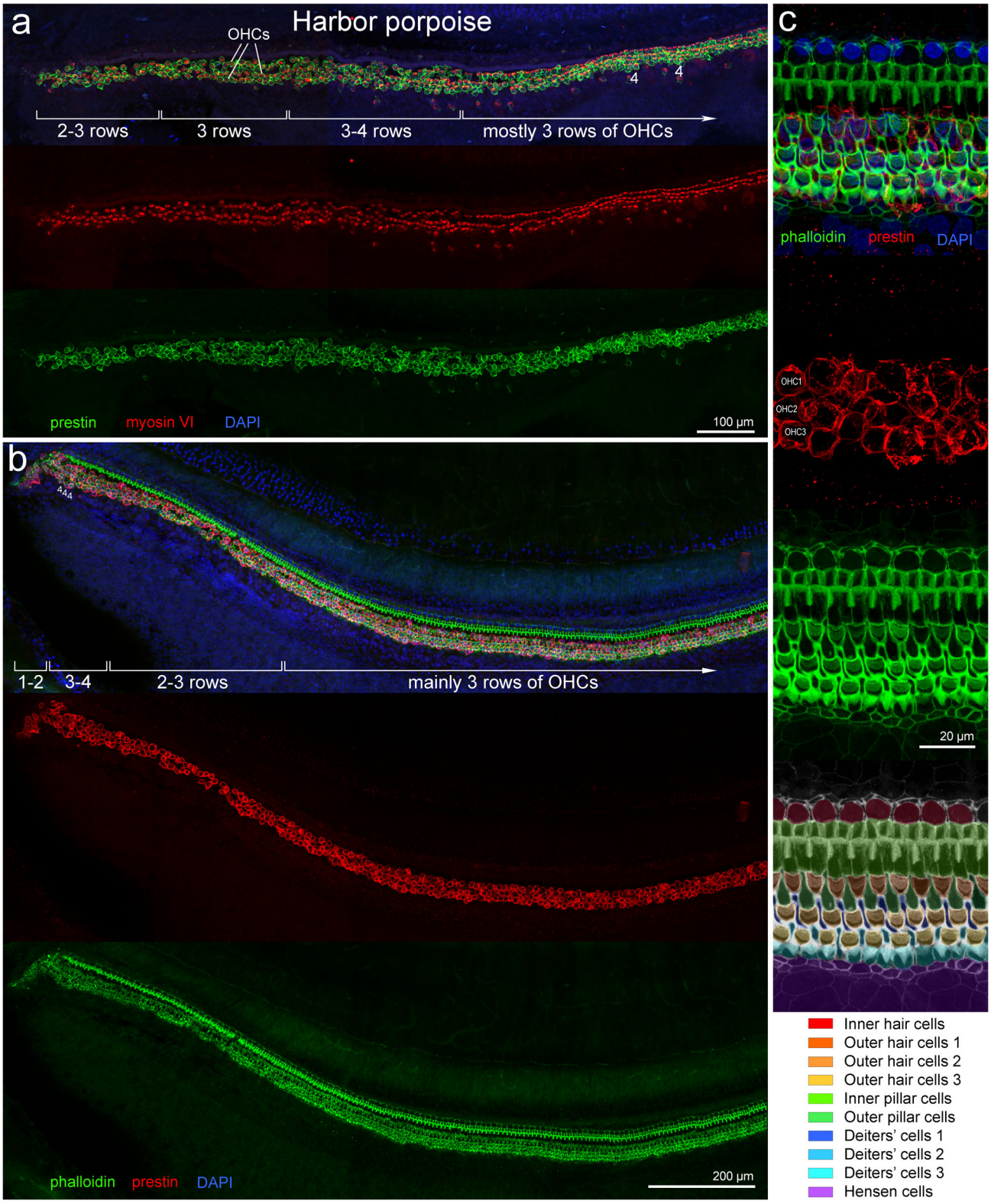

FIGURE 4 Legend on next page.

the left cochlea from 400 to 580 μm and between 840 and 900 μm the OHC3s were not well preserved and precluded ultrastructural evaluation.

3.4 | Pygmy sperm whale

With the exception of a 20 μm segment, IF analysis of one left ear revealed the presence of the cells of the organ of Corti throughout the apex. However, the first region of the organ of Corti was not readily apparent and it is possible that immunofluorescent findings may be indicative of regions closer to the base. In the first 200 μm, the organ of Corti was formed by two or three rows of OHCs (Figures 2 and 8). From this point onward, there was the typical three-row alignment of OHCs.

3.5 | Beluga whale

All the beluga whales from this study were adults. Five ears from three individuals were collected from the Arctic, while three ears from two whales were from captive animals. The disposition of hair cells in the apex varied greatly (Figure 3). While some ears showed the three-row pattern of OHCs throughout nearly the whole apex (cet 336A, Figure 9a), others displayed OHCs from a fourth row in a region, 440 μm long (from 440 to 880 μm from the apex in individual cet 344A). However, the majority of the ears showed the same pattern as described for the other species in this study: a first segment of the apex with two or three rows of OHCs, transitioning to three rows of OHCs starting in the last 380–740 μm, with an average of 440 μm in at least 70% of the cases (Figure 3). Figure 9b,c shows the disposition of the sensory cells and supporting cells in higher magnification. In the best preserved individuals, a narrow groove (white dotted lines in Figure 9) separated the Deiters' from the Hensen cells. Figure 9d shows the morphology of the organ of Corti in the upper basal turn, for comparison with the apex.

The three pairs of ears from the same individuals (cet 344, cet 340, and cet 419) showed large intraindividual variability as well with differences in the arrangement of OHCs between right (A) and left (B) ears (Figure 3). Since the samples from the wild belugas were fresher (perfused within 3.25 hr postmortem), all their apical regions were complete or nearly complete, and the IHCs were observed throughout the apex (Figures 9 and 10).

In the other species, OHC1 and OHC2 were consistently present in the apex in the majority of the cases; whereas, the third row was not always identified. In contrast, six examined ears from belugas lacked scattered OHC1 or OHC2 (Figures 3 and arrows in Figure 9c).

3.6 | Common findings among species

In the best preserved cochleas analyzed by SEM and in one sample labeled with phalloidin by IF, the different types of supporting and sensory cells could be distinguished (highlighted in different colors in Figures 4c, 5b, 6b, 9b,c). Usually, when two rows of OHCs were observed, OHC1 and OHC2 were present, as well as Deiters' cells 1 and 2, with no morphologic evidence of Deiters' cells 3 (Figures 5b, 6b, and 9b). Conversely, when three rows of OHCs were observed, there were also three rows of Deiters' cells identified (Figures 4c, 5b, 6b, and 9c).

4 | DISCUSSION

4.1 | There is a high interindividual variability in the disposition of OHCs in the apex

For some of these species (*K. breviceps*, *S. attenuata* and *S. longirostris*), this is the first study to describe the disposition of cells of the organ of Corti. Valuable anatomic variations were identified despite the dataset for this

FIGURE 4 Immunofluorescence images of maximum projections from z stacks from the apical cochlea of two juvenile harbor porpoises stranded in The Netherlands and fixed 4 hr postmortem. One sample was fixed with 10% neutral buffered formalin (individual cet 404, (a)) and the other with 4% paraformaldehyde (individual cet 426, (b,c)). The apex is located at the left side of the figure. (a) The flat preparations were labeled with anti-prestin antibody (green) that labels outer hair cells (OHCs), anti-myosin VI antibody (red) that labels inner (IHCs) and OHCs, and DAPI (blue). There is an area of transition between two, three and four rows of OHCs, followed by the typical formation of three rows of OHCs (with a few cells forming a fourth row in a couple of locations). (b) The first transition region at ~440 μm first displayed one to two rows, followed by three to four rows, and finally two to three rows. After that, the typical three-row pattern of OHCs was shown. In (b,c), the surface preparation was labeled with phalloidin (green), anti-prestin antibody (red) and DAPI. (c) High magnification of the organ of Corti of the apical turn, slightly after the first millimeter. Phalloidin labeling is ideal for identifying the reticular lamina of the different cell types of the organ of Corti. Different types of hair cells and supporting cells were colored in the image from the phalloidin labeling

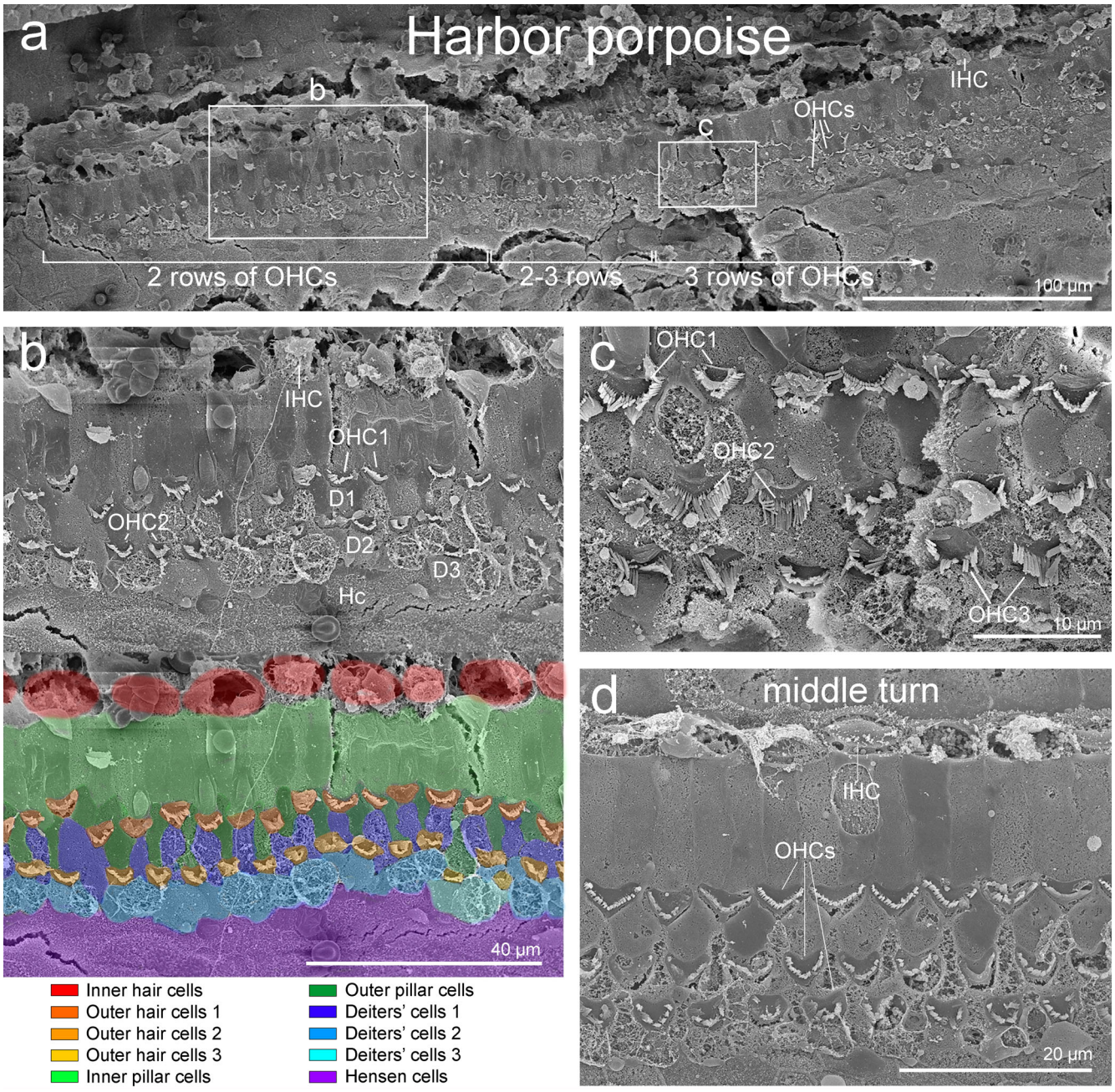

FIGURE 5 (a) Apical region of the cochlea of a 5-year-old nonreleasable harbor porpoise *Phocoena phocoena* from the Vancouver Aquarium (Canada, individual cet 415), fixed 10–12 hr postmortem, using scanning electron microscopy (apex toward the left side). Initially, an area with two rows of outer hair cells (OHC1 and OHC2) is shown in the first 200 µm, followed by a transitional area with an alternation of two and three rows of OHCs (70 µm). A consistent organ of Corti formed by three rows of OHCs was visible from this point onward. (b,c) Higher magnifications of the areas indicated in (a). Panels (a–c) are modified from Morell et al. (2017). (d) Organ of Corti of the middle turn from individual cet 401, fixed around 16 hr postmortem. D, Deiters' cells, Hc, Hensen cells

study being unbalanced in terms of number of individuals per species. While there were several individuals from harbor porpoises and belugas, there was only one spinner dolphin, one pantropical spotted dolphin and one pygmy sperm whale. Although it was not possible to study interindividual variability in these three species, they were included in this study due to the age class of the animals, the preservation status of their cochlea, or the maximum hearing sensitivity of the species.

The collection of ears from neonates or young animals was prioritized. Although neonates can display congenital malformations, this age class is less likely to have damage due to noise, ototoxic drug exposure, heavy metal accumulation, age-related hearing loss, or chronic

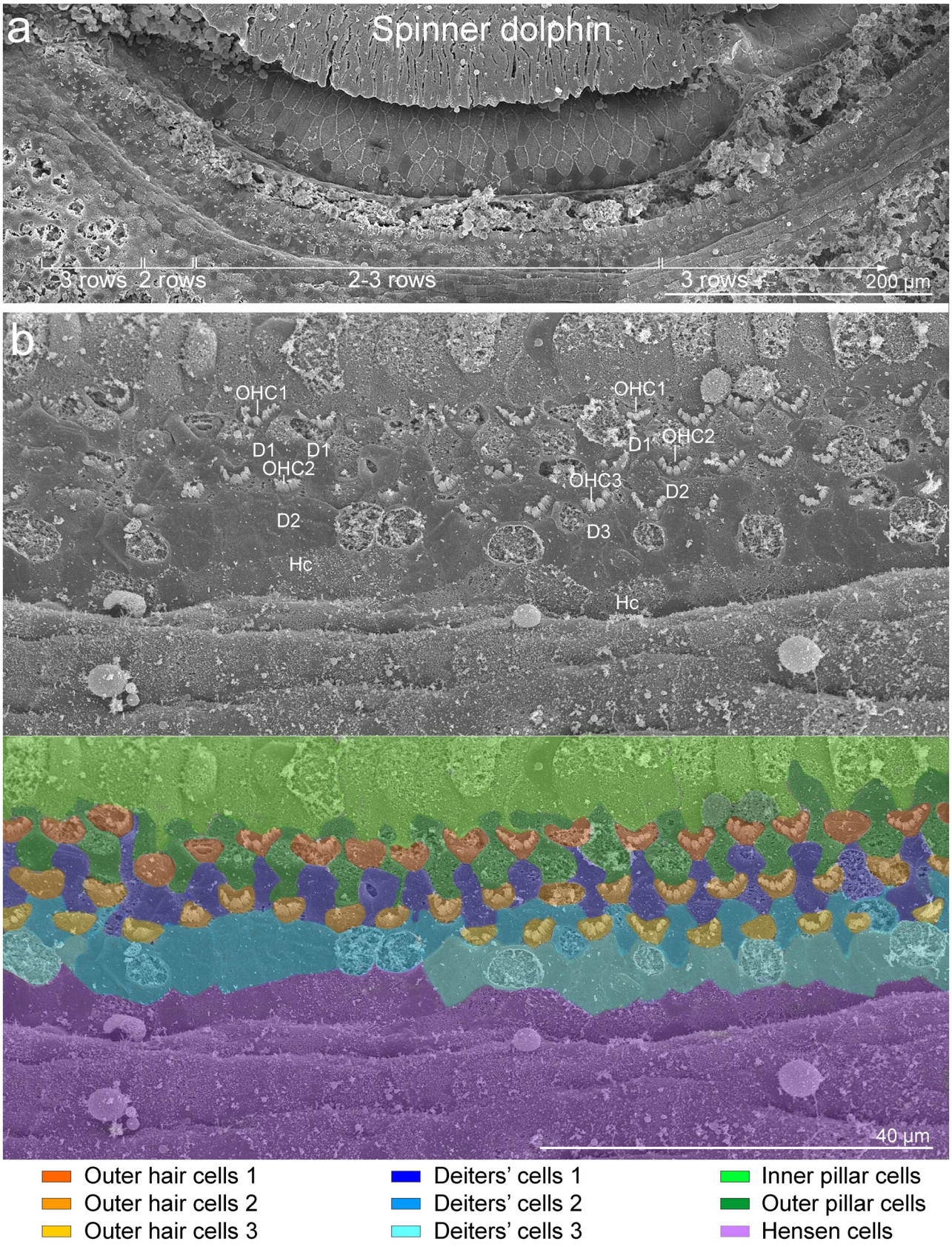

FIGURE 6 Legend on next page.

infectious disease. Some of these perturbations, such as age or exposure to ototoxic drugs, initially affect the base of the cochlea, where the highest frequencies are encoded (see review by Wang & Puel, 2018). However, hair cell loss can also occur in addition in the apical region of the cochlea in aged rats and in senescence-accelerated models of mice (Menardo et al., 2012). As a result, neonates are considered the best candidates to define the "normal" apex variability for the species.

We considered including a single ear from spinner dolphin because it was a fresh neonate with an estimated age of between 1 and 1.5 months, the cochlear epithelium was well preserved (Figure 6) and the apex was complete. The pantropical spotted dolphin was also a young individual (age estimated around 1 year old) with complete sensory epithelium of the apex in the right ear and the organ of Corti was sufficiently well preserved for ultrastructural evaluation. The pygmy sperm whale, however, was an adult. This animal was included in the study because the ear was very fresh (fixed between 2 and 3 hr postmortem).

In addition, the species were selected according to their frequency of maximum hearing sensitivity, to be able to cover a large spectrum of hearing capabilities of toothed whales. Toothed whales can be divided into two hearing groups according to direct measurements of hearing capabilities, anatomy-based predictions of their hearing range (Racicot, Gearty, Kohno, & Flynn, 2016) and characteristics of their echolocation signals. The two proposed hearing groups are: very high frequency specialists (with frequencies of maximum hearing sensitivities exceeding 100 kHz for some species) and high frequency specialists (see Southall et al., 2019 for review). Pygmy sperm whales and harbor porpoises are very high frequency specialists. Pygmy sperm whales have a maximum of hearing sensitivity between 90 and 150 kHz (Ridgway & Carder, 2001) and harbor porpoises between 120 and 130 kHz (Kastelein, Helder-Hoek, & van de Voorde, 2017; Ruser et al., 2016). Conversely, belugas are more sensitive to lower frequencies ranging from 45 to 80 kHz (Mooney et al., 2018). The maximum hearing sensitivity measured for spinner dolphin was 40 and 10 kHz for pantropical spotted dolphin (Greenhow, 2013). However, the value for the pantropical spotted dolphin was likely not representative of the species. This animal had severe hearing loss with no responses detected at and above 20 kHz by electrophysiological methods and high increase of hearing thresholds measured above 14 kHz by behavioral methods (Greenhow, 2013). As a result, patterns of OHCs in the apex of five species with different hearing sensitivities were compared in this study.

Results from harbor porpoise and beluga cochleas revealed that there was interindividual variability (Figures 2 and 3), emphasizing the importance of having multiple individuals per species to establish a "normal" (i.e., undamaged) anatomical baseline. Having harbor porpoises from different age classes might have added interindividual variability. However, it provided information between typical variability displayed from neonates and examples of potential hair cell death throughout the life of the individuals. Thus, scattered loss of hair cells (arrows in Figure 9c) could be due to age (or some perturbations that the animal has suffered during its lifetime) and not necessarily represent a normal species variation of the apex.

With respect to the belugas, all individuals were adults, and the inclusion of three pairs of cochleas facilitated intraindividual comparisons. Variability was identified in the distribution of OHCs between the right and left ears of individual belugas since they did not show identical disposition. However, the source of this variability is unclear at this moment. In older individuals, differences in OHC arrangement in right and left ears may be accentuated because of age-related OHC loss, although the juvenile pantropical spotted dolphin also showed differences between the right and left ears (Figure 3). More pairs of ears should be included in similar analyses to draw more significant conclusions on intraindividual variability of the distribution of OHCs.

The techniques used for visualization (SEM and IF) gave complementary information on the different structures of the cells of the organ of Corti. High resolution SEM provided information at the ultrastructural level of the reticular lamina and stereocilia of the sensory and supporting cells of the organ of Corti. Conversely, the selection of antibodies presented in this study was to

FIGURE 6 Scanning electron micrographs of the right cochlea of a neonate spinner dolphin (*Stenella longirostris*) stranded in La Reunion, France (individual cet 414), and fixed between 6 and 12 hr postmortem. (a) General image of the apex (<1 mm). The beginning of the apex is located to the left. The organ of Corti was formed by three rows of outer hair cells (OHCs) in the first 80 μm with scattered cells forming a fourth row, then a two-row pattern was observed for the next 80 μm, followed by a region of alternation of two and three rows up to 660 μm from the apex. A three-row pattern of OHCs was observed beyond 660 μm. (b) Higher magnification of an area where the organ of Corti is formed by two rows of OHCs on the left, and by three rows of OHCs on the right. When two rows of OHCs were present, there were also only two rows of Deiters' cells (D). The OHCs and supporting cells were colored in the panel below to highlight their arrangement within the organ of Corti. Hc, Hensen cells

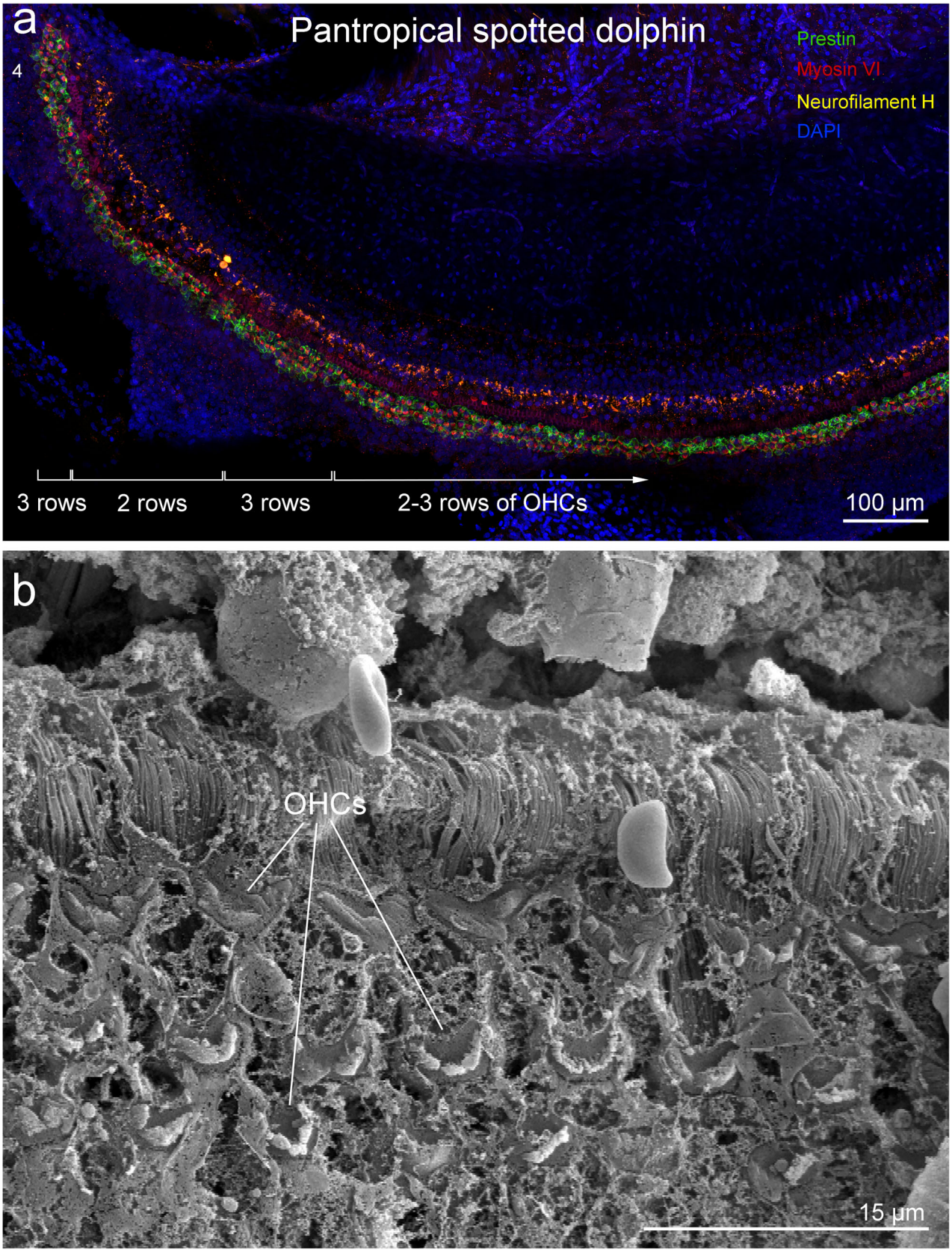

FIGURE 7 Legend on next page.

enhance visualization of the length of sensory cells. Phalloidin labeling in a sample that was fixed with 4% paraformaldehyde proved an ideal way to distinguish the arrangement of sensory cells and the different types of supporting cells (Figure 4b,c at higher magnification). However, both techniques have some inherent limitations. The processing of cochlea for SEM required full dehydration and, in some cases, there were artifactual tears of the basilar membrane, which is thinner and larger in the apical region (Ketten, 1992; Morell, 2012). In some cases, cellular debris attributed to decomposition or hemorrhages overlaid the reticular lamina, which hampered the visualization of stereocilia or the apical membrane of the sensory cells. These limitations are the main reasons why there was incomplete information of the apex in some of the examined samples. In addition, IF requires a more challenging dissection since the half turns of the cochlear spiral have to be flat to mount onto slides, although the subsequent processing is milder on the tissue than for SEM. The apical turn is the most difficult segment of the cochlea to dissect. Moreover, autolysis may denature sensory cell wall epitopes and hamper antibody binding, thus preventing the labeling of some OHCs and resulting in false negative results. Thus, caution should be used in interpreting IF-stained ears from individuals that are not that fresh (e.g., cet 420). We did not use antibodies to specifically detect Deiters' or Hensen cells, and it was not possible to differentiate among different types of supporting cells with our experimental design for IF, with the exception of cet 426 whose cochlea was labeled with phalloidin and anti-prestin antibody. As previously discussed in Morell, Vogl, et al. (2020), positive labeling of phalloidin was not found in tissue fixed with 10% neutral buffered formalin, which is the most commonly used fixative among stranding networks worldwide. Methanol that is often present in formalin denatures F-actin (Gonsior, Platz, Buchmeier, Scheer, & Jockusch, 1999), likely preventing phalloidin labeling. There is a need to find alternative antibodies that recognize cetacean cochlea, to differentiate among supporting cell types, both at the level of the reticular lamina and along their length. Regardless of the technique used for analysis, the limiting factor in the cochleas used in this study was the time between death of the animal and fixation of the inner ear. We observed fewer postmortem decomposition artifacts in the freshest samples, allowing an easier identification of the different cell types that form the organ of Corti.

To summarize, in those species where several individuals were compared, we observed interindividual and intraindividual variability in the disposition of OHCs in the apex. This variability might therefore be considered natural for these species, although it is likely that age and/or some perturbations that the animal has suffered during its lifetime lead to the death of OHCs and the variability we observed.

4.2 | The number of rows of Deiters' cells can be a good indicator to distinguish between normal and pathological features

The ultrastructural features of supporting cells are different among cell types, and it is possible to distinguish between pillar, Deiters' and Hensen cells by location and quantity of microvilli. Ultrastructural studies in guinea pigs revealed that Hensen cells have numerous microvilli along the surface facing the scala media (Bredberg et al., 1972). The microvilli concentration is denser near the cell junctions. In contrast, the phalangeal processes of Deiters' cells have relatively few microvilli and are more evenly distributed. The outer pillar cells have even fewer microvilli, which are close to the periphery of the cells. The inner pillar cells typically have very few microvilli.

In the best-preserved samples of our study and particularly evident in beluga (Figure 9), Deiters' and Hensen cells could be distinguished in SEM micrographs (Figures 5b and 6b). In belugas, Deiters' and Hensen cells were delimited by a narrow groove (white dotted line in Figure 9b,c), rendering a clear distinction among these two supporting cell types. Colored panels in Figures 4c, 5b, 6b, 9b,c indicate the location of individual sensory and supporting cells.

The SEM revealed that when two rows of OHCs (usually OHC1 and OHC2) were present, there were also two rows of Deiters' cells in most cases (Figures 5b, 6b, and 9b). A similar, even more extreme, pattern was observed in the

FIGURE 7 Apical region of the cochlea of a juvenile female pantropical spotted dolphin (*Stenella attenuata*) stranded in La Reunion, France, and fixed 2–3 hr postmortem (individual cet 446). (a) Immunofluorescence images of maximum projections of z-stacks of the right apical turn (apex on the left). The flat preparations were labeled with anti-prestin antibody (green) that labels outer hair cells (OHCs), anti-myosin VI antibody (red) that labels inner (IHCs) and OHCs, and DAPI (blue). In the first region, there were three rows of OHCs, followed by two rows, then three rows, and finally an alternation between two and three rows of OHCs. (b) Scanning electron micrograph of the left apex showing the organ of Corti formed by three rows of OHCs. The preservation status of the tissue was inferior to that of the other specimens

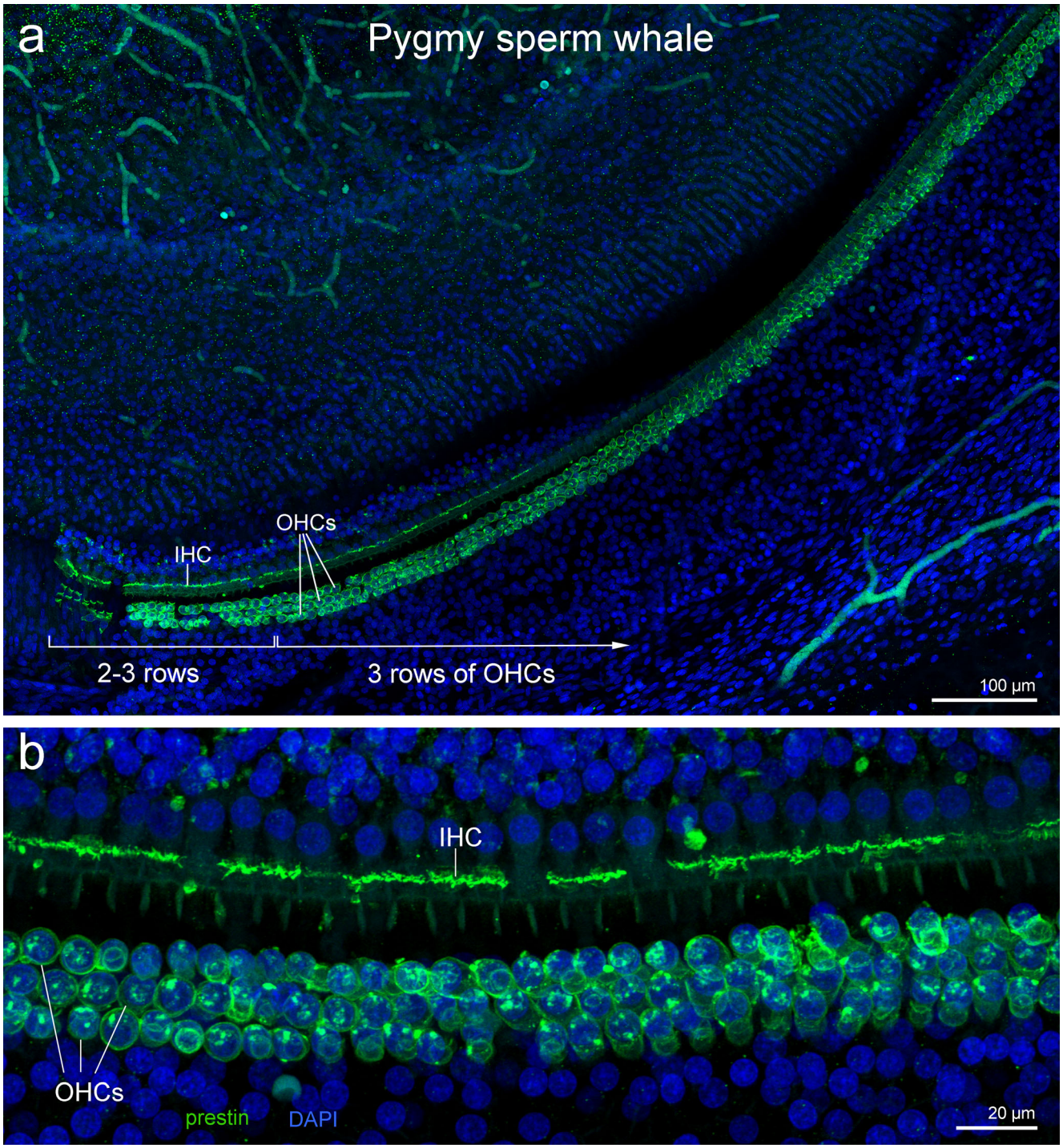

FIGURE 8 Immunofluorescence image of the maximum projection of the left cochlea of an adult male pygmy sperm whale (*Kogia breviceps*) stranded in North Carolina (individual cet 434). The ear was fixed 2–3 hr postmortem. a) The beginning of the apex is on the left. The flat preparation was labeled with anti-prestin antibody (green) and DAPI (blue). The initial 200 µm were observed to have an alternation of two and three rows of outer hair cells (OHCs), followed by a three-row pattern throughout the rest of the apex. It is possible that there was a first region with no information of the organ of Corti since it was challenging to determine its beginning. b) High magnification of the organ of Corti of the apical turn, slightly after the first millimeter. IHC: inner hair cell

apex of the mole rat (Raphael et al., 1991). At the extreme apex, there were no OHCs or Deiters' cells and the outer pillar cells were contiguous with Hensen cells. Thus, our study further contributes to the observation that the OHCs and the Deiters' cells are paired together. This discovery in cetacean species expands our current knowledge from

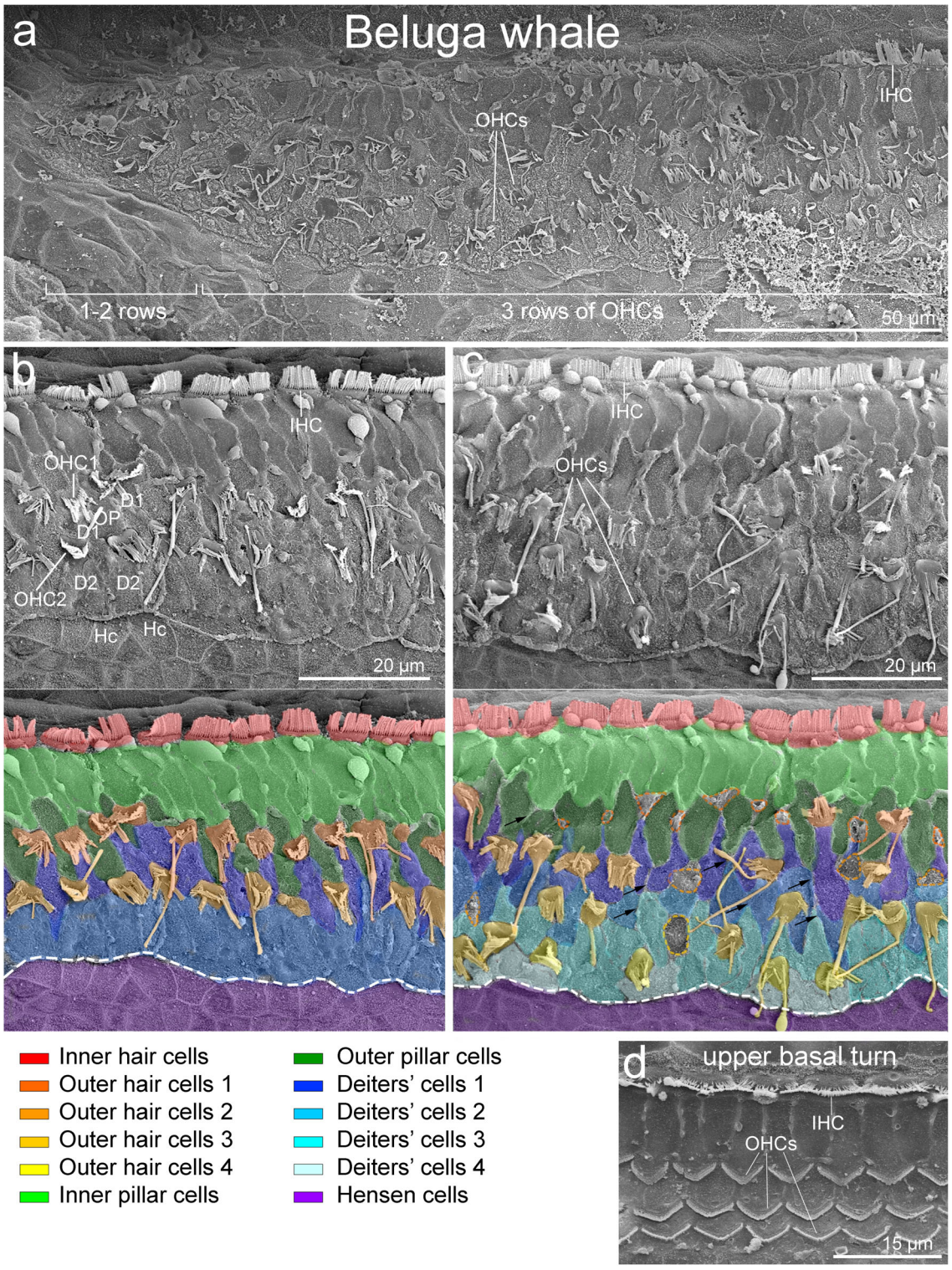

FIGURE 9 Scanning electron micrographs of the cochlea of adult belugas (*Delphinapterus leucas*) from the Canadian Arctic. (a) General image of the first 150 µm of the apex (located to the left) of the right ear from individual cet 336, fixed 3.25 hr postmortem and showing a pattern of one to two rows of outer hair cells (OHCs) in the first 30 µm, followed by a three-row pattern. (b,c) Close-up images of the left cochlea from individual cet 344, fixed between 2 and 3 hr postmortem. The narrow groove has been highlighted with a white dotted line. In (b), there is a region with two rows of OHCs, which also displays only two rows of Deiters' (D) cells. In (c), there are some missing OHCs (highlighted with arrows), which were typically observed to be missing from the third row in other species, but in the adult beluga examples, there was scattered loss of OHCs in the first and second row as well. There were potential remains of OHCs marked with a discontinued line. In (b,c), hair cells and supporting cells were colored in the panel below to highlight their arrangement within the organ of Corti. (d) Organ of Corti of the upper basal turn of the same individual as panel (a) for comparison. IHC, inner hair cell; OP, outer pillar cell

terrestrial mammals (Lenoir et al., 1987; Raphael et al., 1991; Vater & Lenoir, 1992; Vater & Siefer, 1995).

There is high variability in the disposition of the row pattern of OHCs in the first 200 up to 840 μm from the apex. However, we propose that the paired OHC-Deiters' cell can be a good indicator of distinguishing between normal anatomic variability and pathologic processes. For example, when there are two rows of OHCs and two rows of Deiters' cells, it can be considered part of the normal variability of the apex (as shown in the neonate spinner dolphin cet 414, Figure 6b, the adult harbor porpoise cet 415, Figure 5b, or the adult beluga cet 344, Figure 9b). Whereas, when there are two rows of OHCs and three rows of Deiters' cells, then scar formation (as evidence of hair cell death by apoptosis) can be inferred (arrows in Figure 9c).

This pattern of two rows of OHCs together with only two rows of Deiters' cells in the apex was also shown in a study on the development of the cochlea of echolocating horseshoe bats (*Rhinolophus rouxii*, Vater, Lenoir, & Pujol, 1997). This indicates that other echolocating species also show the same pattern, even during development. Conversely, studies on the postnatal development of Deiters' cells in the apical turn of mice during and just after the onset of hearing showed that they had a peak in their activity at Days 10–11 after birth (Berekméri, Fekete, Köles, & Zelles, 2019). This coincides with a critical developmental period for OHCs, when these cells start to express the motor protein prestin that is essential to hearing (Zheng et al., 2000). During the same period, the tectorial membrane releases from the top of the organ of Corti (Lim & Anniko, 1985; Steel, 1983), thus allowing sound-induced OHC activity through stereocilia and tectorial membrane interaction (Lim, 1972; Steel, 1983). In addition, Ceriani et al. (2019) described that OHCs show spontaneous calcium signals that are coordinated

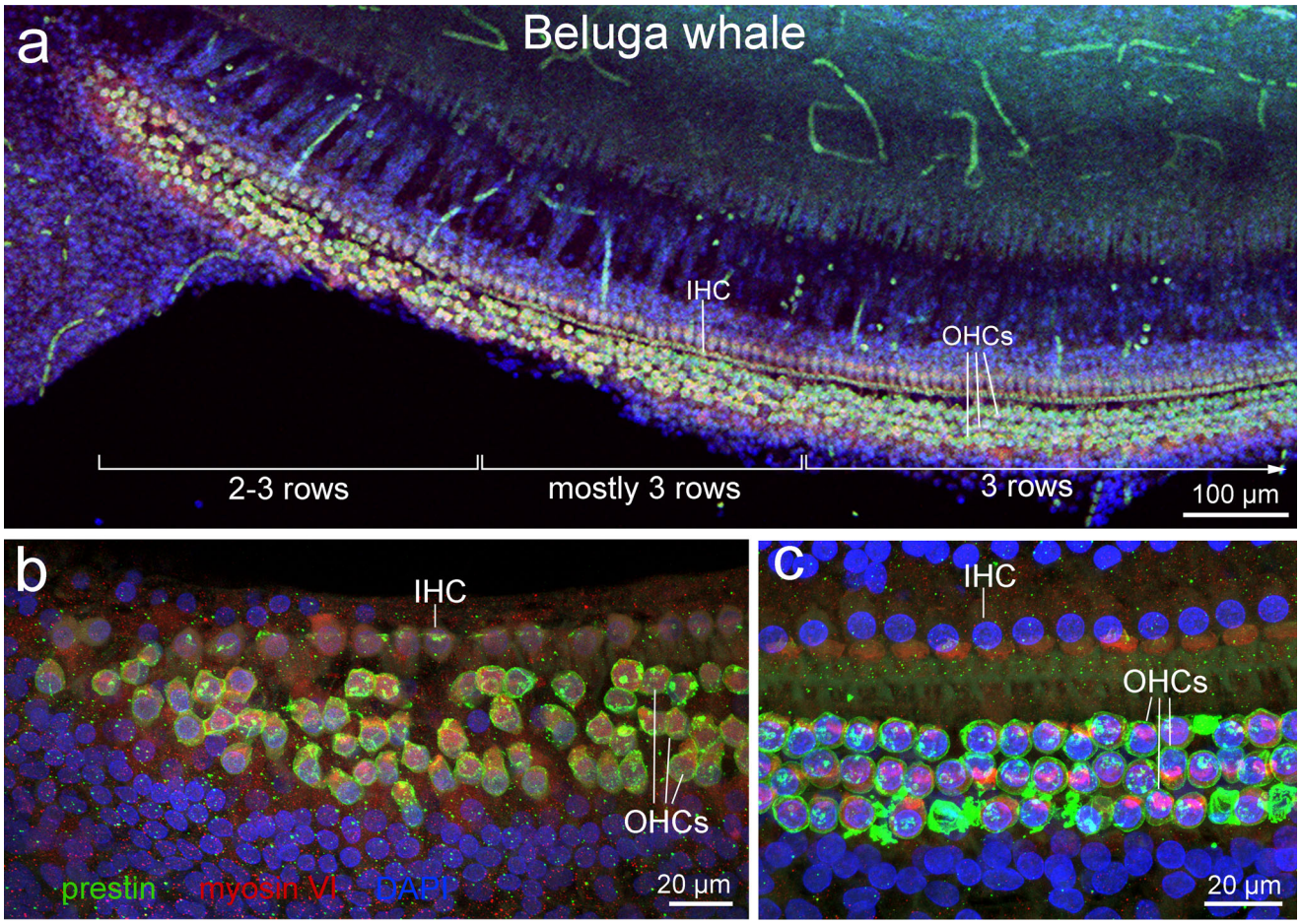

FIGURE 10 Immunofluorescence images of the maximum projection of the right cochlea of an adult male beluga from the Canadian Arctic (individual cet 340). The ear was fixed 1.25 hr postmortem. The beginning of the apex is on the left. The flat preparation was labeled with anti-prestin antibody (green) and DAPI (blue). The initial region up to 240 μm was observed to have an alternation of two and three rows of outer hair cells (OHCs), followed mostly by the three-row pattern, and finishing with the three rows of OHCs throughout the rest of the apex. (b) Higher magnification of the first cells of the beginning of the apex. (c) Higher magnification of the cells of the organ of Corti of the apical turn, slightly over the first millimeter. IHC: inner hair cell

by the neighboring Deiters' cells in mice, with a maximal OHC activity in Days 0 and 1 in the basal and apical turns, respectively. Although harbor porpoises have full hearing capabilities at birth (Wahlberg, Delgado-García, & Kristensen, 2017) and therefore may have a different postnatal mechanism than mice, it is possible that the main activity of OHCs during development is also related to the associated Deiters' cells.

Most of the individuals of this study (16 out of 23) are expected to be "normal", although we only have a full behavioral audiogram (250 Hz to 160 kHz) of one harbor porpoise (individual cet 401, porpoise Pp02 in Kastelein, Hoek, de Jong, & Wensveen, 2010). Kastelein et al. tested the hearing capabilities of this individual regularly and it did not show evidence of low-frequency hearing loss before its death. Its audiogram was similar to that of four other individuals of the same species whose audiograms were measured in comparable conditions and with similar methods (Kastelein et al., 2017). Extending from the 600 μm level from the apex toward the base in this animal, the relationship between hair cell disposition and hearing capabilities could be assessed, whereas, more apically, these evaluations could not be undertaken. We did not have full behavioral audiograms for the remaining samples. Some belugas, such as individual cet 344 (Figure 9b, c), displayed the formation of giant stereocilia of OHCs. The formation of giant stereocilia has been described as a consequence of noise/ototoxic drug exposure (Avinash, Nuttall, & Raphael, 1993; Bredberg et al., 1972; Chen et al., 2003), though studies in humans also showed the presence of giant stereocilia as a consequence of postmortem autolysis (Wright, 1980) and age (Bredberg et al., 1972; Bullen et al., 2020). Consequently, we could not find evidence to determine the presence of giant stereocilia as a pathological condition in our samples. In addition, the orange dotted shapes in Figure 9c show the difficulty of recognizing the typical OHC shape in regions where those remains could also be part of the reticular lamina of OHCs. In those cases, we applied a conservative approach and did not consider them as pathology. However, the arrows shown in Figure 9c highlight the presence of scars. Six belugas also displayed scattered loss of few OHCs, sometimes in OHC1 and OHC2 (Figure 3). Those cases are considered "not normal" and not within the apical variability of the species, but likely a result of age-related hair cell death. The scattered loss observed in the beluga samples was not necessarily caused by exposure to noise, ototoxic drugs or infectious diseases.

This study highlights the importance of describing "normal" morphological features of ears collected from different demographics to establish baselines of the apex of cetaceans. This information will enhance our understanding of how low frequency man-made noise might affect cetacean hearing. The results of this research suggest that the number of rows of Deiters' cells is a good indicator to distinguish between normal and pathological features in examined cetacean cochleas.

ACKNOWLEDGMENTS

The authors would like to thank Marc Lenoir for his scientific advice and helpful comments on the manuscript, as well as Yehoash Raphael and two anonymous reviewers for their constructive advice. The authors would also like to thank Kevin Hodgson and Derrick Horne (University of British Columbia Bioimaging Facility), Baptiste Monterroso (MRI), Chantal Cazevieille (COMET), Didier Cot (IEM), and Vanessa Auld (UBC) for technical assistance and Ron Kastelein (SEAMARCO) who provided the ears of a harbor porpoise with known audiogram (individual cet 401). Canadian Natural Sciences and Engineering Research Council Discovery grant (grant number: RGPAS 446012-13). Canadian Natural Sciences and Engineering Research Council Accelerator grant (grant number: RGPAN 312039-13). Marie Skłodowska-Curie Individual Post-doctoral Fellowship (grant number: 751284-H2020-MSCA-IF-2016). Open Access funding enabled and organized by Projekt DEAL.

CONFLICT OF INTEREST

The authors declare no conflict of interest.

AUTHOR CONTRIBUTIONS

Maria Morell, **Lonneke L. IJsseldijk**, **Marina Piscitelli-Doshkov**, **Sonja Ostertag**, **Vanessa Estrade**, **Paul Doshkov**, and **Stephen A. Raverty** were in charge of the necropsies from cetaceans and to remove and fix the ears. **Maria Morell**: Performed the inner ear dissection, their preparation for confocal microscopy, SEM, and image interpretation. **Jérôme Bourien**: Performed the statistical analysis. **Martin Haulena** was in charge of the care of the individuals in captivity from this study (cet 415, cet 419, and cet 420). **Maria Morell**, **Lonneke L. IJsseldijk**, **Marina Piscitelli-Doshkov**, **Sonja Ostertag**, **Vanessa Estrade**, **Martin Haulena**, **Paul Doshkov**, **Jérôme Bourien**, **Stephen A. Raverty**, **Ursula Siebert**, **Jean-Luc Puel**, and **Robert E. Shadwick**: Helped with writing and editing the manuscript. **Stephen A. Raverty**, **Ursula Siebert**, **Jean-Luc Puel**, and **Robert E. Shadwick**: Supervised the work and its publication. All authors contributed to the article and approved the submitted version.

ORCID

Maria Morell https://orcid.org/0000-0003-1959-5852
Robert E. Shadwick https://orcid.org/0000-0002-5039-8606

REFERENCES

Avinash, G. P., Nuttall, A. L., & Raphael, Y. (1993). 3-D analysis of F-actin in stereocilia of cochlear hair cells after loud noise exposure. *Hearing Research*, *67*, 139–146.

Berekméri, E., Fekete, A., Köles, L., & Zelles, T. (2019). Postnatal development of the subcellular structures and purinergic signaling of Deiters cells along the tonotopic axis of the cochlea. *Cell*, *8*, 1266.

Bredberg, G., Ades, H. W., & Engstrom, H. (1972). Scanning electron microscopy of normal and pathologically altered organ of Corti. *Acta Oto-Laryngologica*, *73*, 3–48.

Bullen, A., Forge, A., Wright, A., Richardson, G. P., Goodyear, R. J., & Taylor, R. (2020). Ultrastructural defects in stereocilia and tectorial membrane in aging mouse and human cochleae. *Journal of Neurosurgical Sciences*, *98*, 1745–1763.

Callis, G., & Sterchi, D. (1998). Decalcification of bone: Literature review and practical study of various decalcifying agents, methods, and their effects on bone histology. *Journal of Histotechnology*, *21*, 49–58.

Ceriani, F., Hendry, A., Jeng, J., Johnson, S. L., Stephani, F., Olt, J., ... Marcotti, W. (2019). Coordinated calcium signalling in cochlear sensory and non-sensory cells refines afferent innervation of outer hair cells. *The EMBO Journal*, *38*, e99839.

Chen, Y. S., Liu, T. C., Cheng, C. H., Yeh, T. H., Lee, S. Y., & Hsu, C. J. (2003). Changes of hair cell stereocilia and threshold shift after acoustic trauma in Guinea pigs: Comparison between inner and outer hair cells. *ORL*, *65*, 266–274.

Engstrom, B., Borg, E., & Canlon, B. (1984). Morphology of stereocilia on cochlear hair cells after noise exposure. In R. J. Salvi, D. Henderson, R. P. Hamernik, & V. Colletti (Eds.), *Basic and applied aspects of noise-induced hearing loss* (pp. 1–9). New York, NY: Plenum Press.

Erbe, C., Dunlop, R., & Dolman, S. (2018). Effects of noise on marine mammals. In H. Slabbekoorn, R. J. Dooling, A. N. Popper, & R. R. Fay (Eds.), *Effects of anthropogenic noise on animals* (pp. 277–308). New York, NY: Springer Handbook of Auditory Research.

Girdlestone, C., Ng, J., Piscitelli-Doshkov, M., Ostertag, S., Raverty, S. A., Morell, M., & Shadwick, R. E. (2018). Description of cochlear morphology and hair cell variation in the beluga whale. *Arctic Science*, *4*, 279–291.

Gonsior, S. M., Platz, S., Buchmeier, S., Scheer, U., & Jockusch, B. M. (1999). Conformational difference between nuclear and cytoplasmic actin as detected by a monoclonal antibody. *Journal of Cell Science*, *112*, 797–809.

Greenhow, D. (2013). Hearing and echolocation in stranded and captive odontocete cetaceans:1–183.

Henson, M. M., Jenkins, D. B., & Henson, O. W. (1983). Sustentacular cells of the organ of Corti—The tectal cells of the outer tunnel. *Hearing Research*, *10*, 153–166.

Hu, B. H., Guo, W., Wang, P. Y., Henderson, D., & Jiang, S. C. (2000). Intense noise-induced apoptosis in hair cells of Guinea pig cochleae. *Acta Oto-Laryngologica*, *120*, 19–24.

Kastelein, R. A., Helder-Hoek, L., & van de Voorde, S. (2017). Hearing thresholds of a male and a female harbor porpoise (*Phocoena phocoena*). *Journal of the Acoustical Society of America*, *142*, 1006–1010.

Kastelein, R. A., Hoek, L., de Jong, C. A. F., & Wensveen, P. J. (2010). The effect of signal duration on the underwater detection thresholds of a harbor porpoise (*Phocoena phocoena*) for single frequency-modulated tonal signals between 0.25 and 160 kHz. *The Journal of the Acoustical Society of America*, *128*, 3211–3222.

Ketten, D. (1992). The cetacean ear: Form, frequency and evolution. In J. A. Thomas, R. A. Kastelein, & A. Y. Supin (Eds.), *Marine mammal sensory systems* (pp. 56–69). New York, NY: Plenum.

Kikuchi, T., Adams, J. C., Miyabe, Y., So, E., & Kobayashi, T. (2000). Potassium ion recycling pathway via gap junction systems in the mammalian cochlea and its interruption in hereditary nonsyndromic deafness. *Medical Electron Microscopy*, *33*, 51–56.

Lenoir, M., Puel, J. L., & Pujol, R. (1987). Stereocilia and tectorial membrane development in the rat cochlea. A SEM study. *Anatomy and Embryology*, *175*, 477–487.

Lim, D. J. (1972). Fine morphology of tectorial membrane—Its relationship to organ of Corti. *Archives of Otolaryngology*, *96*, 199–215.

Lim, D. J. (1986). Functional structure of the organ of Corti—A review. *Hearing Research*, *22*, 117–146.

Lim, D. J., & Anniko, M. (1985). Developmental morphology of the mouse inner ear: A scanning electron microscopic observation. *Acta Oto-Laryngologica*, *99*, 5–69.

Lim, D. J., & Dunn, D. E. (1979). Anatomic correlates of noise induced hearing loss. *Otolaryngologic Clinics of North America*, *12*, 493–513.

Lim, D. J., & Melnick, W. (1971). Acoustic damage of the cochlea—Scanning and transmission electron microscopic observation. *Acta Oto-Laryngologica*, *94*, 294–305.

Menardo, J., Tang, Y., Ladrech, S., Lenoir, M., Casas, F., Michel, C., ... Wang, J. (2012). Oxidative stress, inflammation, and autophagic stress as the key mechanisms of premature age-related hearing loss in SAMP8 mouse cochlea. *Antioxidants & Redox Signaling*, *16*, 263–274.

Monzack, E. L., & Cunningham, L. L. (2013). Lead roles for supporting actors: Critical functions of inner ear supporting cells. *Hearing Research*, *303*, 20–29.

Mooney, T. A., Castellote, M., Quakenbush, L., Hobbs, R., Gaglione, E., & Goetz, C. (2018). Variation in hearing within a wild population of beluga whales (*Delphinapterus leucas*). *The Journal of Experimental Biology*, *221*(9), jeb171959.

Morell, M. (2012). Ultrastructural analysis of odontocete cochlea: 1–178.

Morell, M., & André, M. (2009). Cetacean ear extraction and fixation protocol. Retrieved from http://www.zoology.ubc.ca/files/Ear_extraction_and_fixation_protocol_UBC.pdf

Morell, M., Brownlow, A., McGovern, B., Raverty, S. A., Shadwick, R. E., & André, M. (2017). Implementation of a method to visualize noise-induced hearing loss in mass stranded cetaceans. *Scientific Reports*, *7*, 41848.

Morell, M., Degollada, E., Alonso, J. M., Jauniaux, T., & Andre, M. (2009). Decalcifying odontocete ears following a routine protocol with RDO®. *Journal of Experimental Marine Biology and Ecology*, *376*, 55–58.

Morell, M., Lenoir, M., Shadwick, R. E., Jauniaux, T., Dabin, W., Begeman, L., ... André, M. (2015). Ultrastructure of the odontocete organ of Corti: Scanning and transmission electron microscopy. *The Journal of Comparative Neurology*, *523*, 431–448.

Morell, M., Raverty, S. A., Mulsow, J., Haulena, M., Barret-Lennard, L., Nordstrom, C., ... Shadwick, R. E. (2020).

Combining cochlear analysis and auditory evoked potentials in a beluga whale with high-frequency hearing loss. *Frontiers in Veterinary Science*, *7*, 534917.

Morell, M., Vogl, W., Ijsseldijk, L., Piscitelli-Doshkov, M., Tong, L., Ostertag, S., ... Shadwick, R. E. (2020). Echolocating whales and bats express the motor protein prestin in the inner ear: A potential marker for hearing loss. *Frontiers in Veterinary Science*, *7*, 429.

National Research Council. (2003). *Ocean noise and marine mammals*. Washington, DC: The National Academies Press.

Racicot, R. A., Gearty, W., Kohno, N., & Flynn, J. J. (2016). Comparative anatomy of the bony labyrinth of extant and extinct porpoises (Cetacea: Phocoenidae). *Biological Journal of the Linnean Society*, *119*, 831–846.

Raphael, Y., & Altschuler, R. A. (2003). Structure and innervation of the cochlea. *Brain Research Bulletin*, *60*, 397–422.

Raphael, Y., Lenoir, M., Wroblewski, R., & Pujol, R. (1991). The sensory epithelium and its innervation in the mole rat cochlea. *The Journal of Comparative Neurology*, *314*, 367–382.

Ridgway, S. H., & Carder, D. A. (2001). Assessing hearing and sound production in cetaceans not available for behavioral audiograms: Experiences with sperm, pygmy sperm, and gray whales. *Aquatic Mammals*, *27*, 267–276.

Ruser, A., Dähne, M., van Neer, A., Lucke, K., Sundermeyer, J., Houser, D. S., ... Teilmann, J. (2016). Assessing auditory evoked potentials of wild harbor porpoises (*Phocoena phocoena*). *The Journal of the Acoustical Society of America*, *140*, 442–452.

Saunders, J. C., Dear, S. P., & Schneider, M. E. (1985). The anatomical consequences of acoustic injury: A review and tutorial. *The Journal of the Acoustical Society of America*, *78*, 833–860.

Simmonds, M. P., Dolman, S. J., Jasny, M., Parsons, E. C. M., Weilgart, L., Wright, A. J., & Leaper, R. (2014). Marine noise pollution—Increasing recognition but need for more practical action. *Journal of Ocean Technology*, *9*, 71–90.

Slepecky, N., Henderson, C., & Saha, S. (1995). Post-translational modifications of tubulin suggest that dynamic microtubules are present in sensory cells and stable microtubules are present in supporting cells of the mammalian cochlea. *Hearing Research*, *91*, 136–147.

Southall, B. L., Finneran, J. J., Reichmuth, C., Nacthigall, P. E., Ketten, D. R., Bowles, A. E., ... Tyack, P. L. (2019). Marine mammal noise exposure criteria: Updated scientific recommendations for residual hearing effects. *Aquatic Mammals*, *45*, 125–232.

Spicer, S. S., & Schulte, B. A. (1994). Ultrastructural differentiation of the first Hensen cell in the gerbil cochlea as a distinct cell type. *The Anatomical Record*, *240*, 149–156.

Spicer, S. S., & Schulte, B. A. (1998). Evidence for a medial K‡$^{+}$ recycling pathway from inner hair cells. *Hearing Research*, *118*, 1–12.

Steel, K. P. (1983). The tectorial membrane of mammals. *Hearing Research*, *9*, 327–359.

Vater, M., & Lenoir, M. (1992). Ultrastructure of the horseshoe bat's organ of Corti I. Scanning electron microscopy. *The Journal of Comparative Neurology*, *318*, 367–379.

Vater, M., Lenoir, M., & Pujol, R. (1997). Development of the organ of Corti in horseshoe bats: Scanning and transmission electron microscopy. *The Journal of Comparative Neurology*, *377*, 520–534.

Vater, M., & Siefer, W. (1995). The cochlea of *Tadarida brasiliensis*: Specialized functional organization in a generalized bat. *Hearing Research*, *91*, 178–195.

Wahlberg, M., Delgado-García, L., & Kristensen, J. K. (2017). Precocious hearing in harbour porpoise neonates. *Journal of Comparative Physiology. A, Neuroethology, Sensory, Neural, and Behavioral Physiology*, *203*, 121–132.

Wang, J., & Puel, J. L. (2018). Toward cochlear therapies. *Physiological Reviews*, *98*, 2477–2522.

Wever, E. G., McCormick, J. G., Palin, J., & Ridgway, S. H. (1971a). Cochlea of dolphin, *Tursiops truncatus*—General morphology. *Proceedings of the National Academy of Sciences of the United States of America*, *68*, 2381–2385.

Wever, E. G., McCormick, J. G., Palin, J., & Ridgway, S. H. (1971b). Cochlea of dolphin. 3. *Tursiops truncatus*—Hair cells and ganglion cells. *Proceedings of the National Academy of Sciences of the United States of America*, *68*, 2908–2912.

Wever, E. G., Ridgway, S. H., Palin, J., & McCormic, J. G. (1972). Cochlear structure in dolphin, *Lagenorhynchus obliquidens*. *Proceedings of the National Academy of Sciences of the United States of America*, *69*, 657–661.

Wright, A. (1980). Scanning electron microscopy of the human cochlea—Postmortem autolysis artefacts. *Archives of Oto-Rhino-Laryngology*, *228*, 1–6.

Zheng, J., Shen, W., He, D. Z. Z., Long, K. B., Madison, L. D., & Dallos, P. (2000). Prestin is the motor protein of cochlear outer hair cells. *Nature*, *405*, 149–155.

How to cite this article: Morell, M., IJsseldijk, L. L., Piscitelli-Doshkov, M., Ostertag, S., Estrade, V., Haulena, M., Doshkov, P., Bourien, J., Raverty, S. A., Siebert, U., Puel, J.-L., & Shadwick, R. E. (2021). Cochlear apical morphology in toothed whales: Using the pairing hair cell—Deiters' cell as a marker to detect lesions. *The Anatomical Record*, 1–21. https://doi.org/10.1002/ar.24680